Deep-Sea Research I 101 (2015) 98–109

Contents lists available at ScienceDirect

Deep-Sea Research I

journal homepage: www.elsevier.com/locate/dsri

Water mass transformation in the Iceland Sea

Kjetil Våge [a,*], G.W.K. Moore [b], Steingrímur Jónsson [c,d], Héðinn Valdimarsson [d]

[a] Geophysical Institute, University of Bergen and Bjerknes Centre for Climate Research, Bergen, Norway
[b] University of Toronto, Toronto, Canada
[c] University of Akureyri, Akureyri, Iceland
[d] Marine Research Institute, Reykjavik, Iceland

ARTICLE INFO

Article history:
Received 7 October 2014
Received in revised form
12 February 2015
Accepted 3 April 2015
Available online 13 April 2015

Keywords:
Iceland Sea
Open-ocean convection
North Icelandic Jet
Denmark Strait Overflow Water
Atlantic Meridional Overturning Circulation
Cold air outbreak

ABSTRACT

The water mass transformation that takes place in the Iceland Sea during winter is investigated using historical hydrographic data and atmospheric reanalysis fields. Surface densities exceeding $\sigma_\theta = 27.8$ kg/m^3, and hence of sufficient density to contribute to the lower limb of the Atlantic Meridional Overturning Circulation via the overflows across the Greenland-Scotland Ridge, exist throughout the interior Iceland Sea east of the Kolbeinsey Ridge at the end of winter. The deepest and densest mixed layers are found in the northwest Iceland Sea on the outskirts of the basin's cyclonic gyre, largely determined by stronger atmospheric forcing near the ice edge. Much of the accumulated wintertime heat loss in that region takes place during a few extreme cold air outbreak events. Only a small number of hydrographic profiles (2%) recorded mixed layers sufficiently dense to supply the deepest part of the North Icelandic Jet, a current along the slope off northern Iceland that advects overflow water into the Denmark Strait. However, low values of potential vorticity at depth indicate that waters of this density class may be ventilated more regularly than the direct observations of dense mixed layers in the sparse data set indicate. A sudden increase in the depth of this deep isopycnal around 1995 suggests that the supply of dense water to the North Icelandic Jet, and hence to the densest component of the Atlantic Meridional Overturning Circulation, may have diminished over the past 20 years. Concurrent reductions in the turbulent heat fluxes and wind stress curl over the Iceland Sea are consistent with a decrease in convective activity and a weakening of the cyclonic gyre, both of which could have caused the increase in depth of these dense waters.

1. Introduction

The water mass transformation that takes place within the Nordic Seas, at the northern extremity of the Atlantic Meridional Overturning Circulation (AMOC), impacts the world ocean and is of key importance for the North Atlantic climate system (e.g. Gebbie and Huybers, 2010; Rhines et al., 2008). Warm, saline Atlantic waters flow northward across the Greenland-Scotland Ridge into the Nordic Seas, release heat to the atmosphere, and the resulting densified waters return southward through gaps in the ridge as overflow plumes. While the overflow transport is about evenly divided east and west of Iceland, the largest overflow plume and the densest contribution to the lower limb of the AMOC passes through the Denmark Strait between Greenland and Iceland (Fig. 1, Jochumsen et al., 2013).

The winter mean climate of the subpolar North Atlantic is dominated by a large-scale pressure dipole known as the North Atlantic Oscillation (NAO) with the Icelandic Low and Azores High being its centers of action (Hurrell, 1995; Hurrell and Deser, 2009). The NAO is considered to be in its positive state when the sea level pressure is anomalously high (low) in the southern (northern) center of action. In its positive state, there is enhanced westerly flow across the mid-latitudes of the North Atlantic. The Iceland Sea is situated in the trailing trough that extends north-eastwards from the Icelandic Low towards the Barents Sea (Serreze et al., 1997). Along this trough there is a secondary low-pressure center known as the Lofoten Low that has a climatological center to the west of northern Norway near 72°N, 14°E (Jahnke-Bornemann and Bruemmer, 2009). The pressure dipole consisting of the Icelandic and Lofoten Lows is known as the Icelandic Lofoten Dipole (ILD). In addition to being important features in the winter mean flow, these two locations are also the primary (Icelandic Low) and secondary (Lofoten Low) maxima in cyclone frequency over the subpolar North Atlantic (Wernli and Schwierz, 2006). Although the NAO and ILD share a common center of action, the Icelandic Low, Jahnke-Bornemann and Bruemmer (2009) have shown that since the 1980s the two pressure dipoles are only weakly correlated.

* Corresponding author.
E-mail address: kjetil.vage@gfi.uib.no (K. Våge).

http://dx.doi.org/10.1016/j.dsr.2015.04.001
0967-0637/

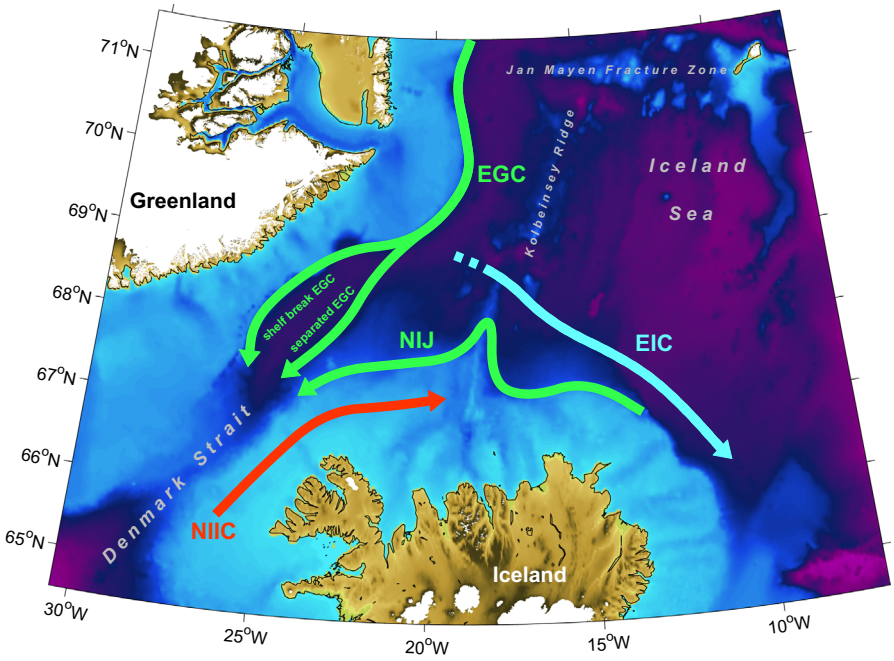

Fig. 1. Bathymetry and schematic circulation in the Iceland Sea. The acronyms are EGC=East Greenland Current; NIJ=North Icelandic Jet; EIC=East Icelandic Current; NIIC=North Icelandic Irminger Current.

The winter mean atmospheric circulation over the subpolar North Atlantic is therefore the result of a complex interplay between these two quasi-independent pressure dipoles. With regard to the Iceland Sea, it appears that the ILD is the primary mode of inter-annual variability (Kelly et al., 1987; Jahnke-Bornemann and Bruemmer, 2009; Moore et al., 2012, 2014). During periods when the Icelandic Low is anomalously deep, southerly flow is established over the Iceland Sea resulting in the advection of warm air and a concomitant reduction in the magnitude of the air–sea heat fluxes (Moore et al., 2012). In contrast, when the Lofoten Low is anomalously deep, the Iceland Sea is under the influence of northerly flow that advects cold air into the region leading to an increase in the magnitude of the sea to air heat fluxes. As a result of this sea-level pressure distribution, the Iceland Sea is situated in a saddle point between the two lows and this leads to a local minimum in air–sea total turbulent heat flux (Moore et al., 2012).

Despite relatively weak atmospheric forcing, oceanic convection takes place in the central Iceland Sea east of the Kolbeinsey Ridge (Fig. 1) and results in the formation of Arctic Intermediate Water (Swift and Aagaard, 1981). Doming isopycnals associated with the presence of a cyclonic gyre (Stefánsson, 1962; Swift and Aagaard, 1981; Voet et al., 2010) facilitate the water mass transformation. Typical late-winter mixed-layer depths are on the order of 200 m (Swift and Aagaard, 1981). The remnants of this convective product are observed during the rest of the year as a cold layer near this depth (e.g. Jónsson, 2007).

The depth of convection in the Iceland Sea is to some extent regulated by the magnitude of the wind stress curl, which has a pronounced influence on the surface salinity (Jónsson, 1992). Fresh conditions during the so-called "ice years" of the late 1960s may have caused a temporary cessation of convection (Malmberg and Jónsson, 1997). At that time the East Icelandic Current, usually an ice free current, transported a larger amount of cold, fresh water of polar origin as well as a substantial amount of drift ice, perhaps brought about by a period of northerly winds and reduced wind stress curl (Dickson et al., 1975; Jónsson, 1992). Over the past three decades a pronounced decline in sea ice concentration in the western Nordic Seas has led to a retreat of the ice edge from the cyclonic gyre in the central Iceland Sea. Simulations with a one-dimensional mixed-layer model predict that the ensuing trend of diminished wintertime atmospheric forcing will reduce the depth and density of the convective product (Moore et al., 2015).

While earlier studies claimed significant contributions from the Iceland Sea to the Denmark Strait overflow plume (e.g. Swift et al., 1980; Livingston et al., 1985; Smethie and Swift, 1989), the current consensus is that the transformation of Atlantic inflow into Denmark Strait Overflow Water (DSOW) occurs primarily within the cyclonic circulation around the margins of the Nordic Seas (Mauritzen, 1996; Eldevik et al., 2009). In this scenario interior convection in the western basins contributes only to a minor extent. It is generally thought that DSOW is mainly advected to the Denmark Strait by the East Greenland Current (e.g. Rudels et al., 2002), but that it contains to various extents an admixture of water formed within the Iceland Sea (Olsson et al., 2005; Tanhua et al., 2005, 2008; Jeansson et al., 2008). The variability among these studies may be related in part to a temporal switching between sources of DSOW (Rudels et al., 2003; Holfort and Albrecht, 2007; Köhl, 2010).

The emphasis on the Iceland Sea as a source of DSOW was renewed with the discovery of a current flowing along the slope north of Iceland in the direction of the Denmark Strait, later called the North Icelandic Jet (NIJ), by Jónsson (1999) and Jónsson and Valdimarsson (2004). They found that the NIJ was potentially of sufficient strength to account for the bulk of the overflow water if some entrainment of ambient water is assumed. Extensive hydrographic/velocity surveys along the slope west and north of Iceland indicate that the NIJ advects both the densest overflow water and a major fraction of the total overflow transport (1.4–1.5 Sv, 1 Sv$=10^6$ m^3/s) into the Denmark Strait (Våge et al., 2011, 2013). Observations and numerical simulations suggest that the NIJ originates along the northern coast of Iceland (Våge et al., 2011; Logemann et al., 2013; Yang and Pratt, 2014). In particular, Våge et al. (2011) hypothesize that it is the deep limb of an overturning loop that involves the boundary current system north of Iceland and water mass transformation in the central Iceland Sea.

Several studies indicate that waters ventilated in the Iceland Sea also take part in the overflows east of Iceland. The Faroe Bank

Channel overflow contains a small contribution from the Iceland Sea in the form of Modified East Icelandic Water (Meincke, 1978; Hansen and Østerhus, 2000; Fogelqvist et al., 2003). Perkins et al. (1998) found at least 0.7 Sv of Arctic Intermediate Water primarily originating from the Iceland Sea to participate in the overflow through the gap in the ridge east of Iceland. There are additional sporadic overflows through other notches along the Iceland-Faroe Ridge that likely contain some water originating from the Iceland Sea (Meincke, 1983). In total the overflow of water ventilated in the Iceland Sea across the Iceland-Scotland Ridge could amount to 0.5–1 Sv, which is consistent with the fluxes of Arctic waters from the Iceland Sea toward the east reported by Jónsson (2007).

The potential contribution from the Iceland Sea to the ventilation of the world ocean via overflows across the Greenland-Scotland Ridge could then be on the order of 2 Sv. This is a substantial fraction of the total overflow, which is generally thought to be about 6 Sv (Østerhus et al., 2008). The motivation for the present study is to shed light on the wintertime water mass transformation that takes places in the Iceland Sea and supplies densified water to the Nordic Seas' overflows. Using a collection of historical hydrographic profiles and atmospheric reanalysis fields we investigate the coupled ocean–atmosphere system in the Iceland Sea region. In particular, we show that waters of sufficient density to contribute to the overflows are produced throughout the central Iceland Sea, investigate the extent to which the densest water masses that are transported by the NIJ and feed the DSOW plume may be formed in this region, and link a decrease in the supply of this dense water to diminishing levels of atmospheric forcing.

2. Data and methods

The historical hydrographic data set used in this study is a new version of that employed by Våge et al. (2013) updated to include the most recent profiles. The data set covers the period 1980 to present and was compiled from various data bases and the Argo global program of profiling floats. Prior to the first deployment of Argo floats in the Iceland Sea in October 2005, the central and northern Iceland Sea was, in particular during winter, sparsely sampled. Additional details about the data set, its quality control, and the gridding procedure can be found in Våge et al. (2013).

In order to determine mixed-layer depths, each of the hydrographic profiles in the historical data set was visually inspected. Two automated routines were employed to identify the base of the mixed layer. The difference criterion method used by Nilsen and Falck (2006) to investigate mixed-layer properties in the Norwegian Sea was adapted to the more weakly stratified conditions in the Iceland Sea. In particular, the potential density near the base of the mixed layer was estimated from the surface properties by subtracting $\Delta T = 0.2\,^{\circ}\mathrm{C}$ (Nilsen and Falck, 2006, used a temperature difference of $\Delta T = 0.8\,^{\circ}\mathrm{C}$). By contrast, the method of Lorbacher et al. (2006) identified the base of the mixed layer as the shallowest extreme in curvature of the temperature profile. For more than half (56%) of the profiles the mixed-layer depth was adequately determined by one or both of these automated routines as judged by visual inspection. The routines performed particularly well on summer and early fall profiles, when the upper ocean was more stratified and there was a pronounced density difference between the base of the mixed layer and the lower part of the profile, but were less accurate during periods of active convection that eroded the stratification. The automated routines were also unable to identify mixed layers isolated from the surface, either in the form of multiple vertically stacked mixed layers or as early stages of restratification, both of which are prevalent also in the Labrador and Irminger Seas during winter (Pickart et al., 2002; Våge et al., 2011). For these remaining profiles (44%) the mixed-layer depth was determined manually following a robust method developed by Pickart et al. (2002) that involves a visual estimation of the mixed-layer extent and the location(s) where the profile permanently crossed outside a two-standard deviation envelope calculated over that depth range.

The atmospheric reanalysis product employed in this study is the global Interim Reanalysis (ERA-I) from the European Centre for Medium Range Weather Forecasts (Dee et al., 2011). We use the 0.75° 6-hourly fields of sea-level pressure, 10 m winds, sea ice, and the turbulent and momentum fluxes for the period from January 1979 to April 2013. Comparison with aircraft and ship observations in the southeast Greenland region shows good agreement with ERA-I (Renfrew et al., 2009; Harden et al., 2011).

The statistical significance of changes in the appearance of time series of interest, such as a linear trend or a transition in mean behavior across a given temporal breakpoint, was assessed using a Monte Carlo significance test that takes into account the temporal auto-correlation characteristics of geophysical time series (Rudnick and Davis, 2003; Moore, 2012). Specifically, 10,000 synthetic time series were generated that shared the same spectral characteristics as the time series in question. These synthetic time series were then used to estimate the probability distribution for the given change in behavior thereby allowing one to estimate the statistical significance of this change in the underlying time series.

3. Wintertime convection in the Iceland Sea

Maps of near-surface wintertime hydrographic properties in the Iceland Sea were first presented by Swift and Aagaard (1981) based on a ship-board survey that took place in late February/early March 1975. They found water denser than $\sigma_\theta = 27.8\ \mathrm{kg/m^3}$, which is typically used to delimit overflow water (e.g. Dickson and Brown, 1994), throughout most of the central Iceland Sea. The densest mixed layers were located in the northern part of the Iceland Sea. Our late winter (February through April) mixed-layer potential densities (Fig. 2a) are slightly lower in the southern part of the Iceland Sea, due to a combination of fresher and warmer waters, but otherwise in qualitative agreement with Swift and Aagaard's (1981) near-surface densities. The corresponding map of mixed-layer depths (Fig. 2b) shows that also the deepest mixed layers tend to be found in the northern Iceland Sea. Mixed layers shallower than 25 m, due to early stages of restratification, were disregarded. While the data nominally span a temporal range of 1980 to present, wintertime observations from the interior Iceland Sea were scarce prior to the deployment of the first Argo floats in late 2005. Most (67%) of the data from the north-central Iceland Sea area outlined in Fig. 2 stem from the period 2005 to present.

It is interesting to note that the deepest and densest mixed layers are found on the outskirts of the Iceland Sea Gyre (Fig. 2). Open-ocean convection is normally thought to take place within cyclonic gyres (e.g. Marshall and Schott, 1999). Doming isopycnals within a gyre bring weakly stratified water closer to the surface resulting in a water column that is more preconditioned for convection (Fig. 3a illustrates that this is the case also in the Iceland Sea). As winter sets in, increased buoyancy loss erodes the near-surface stratification and exposes the weakly stratified water beneath directly to the atmospheric forcing, which allows deeper convection to commence. Off the center of a gyre the water column is less preconditioned, typically resulting in reduced convective activity. We will demonstrate in Section 6 that stronger atmospheric forcing in the northern part of the Iceland Sea is primarily responsible for the deeper and denser mixed layers there, on the outskirts of the gyre.

More intense convection off the center may alter the density structure of the gyre and thereby also its circulation. However, the main seasonal signal in dynamic height of the surface relative to a

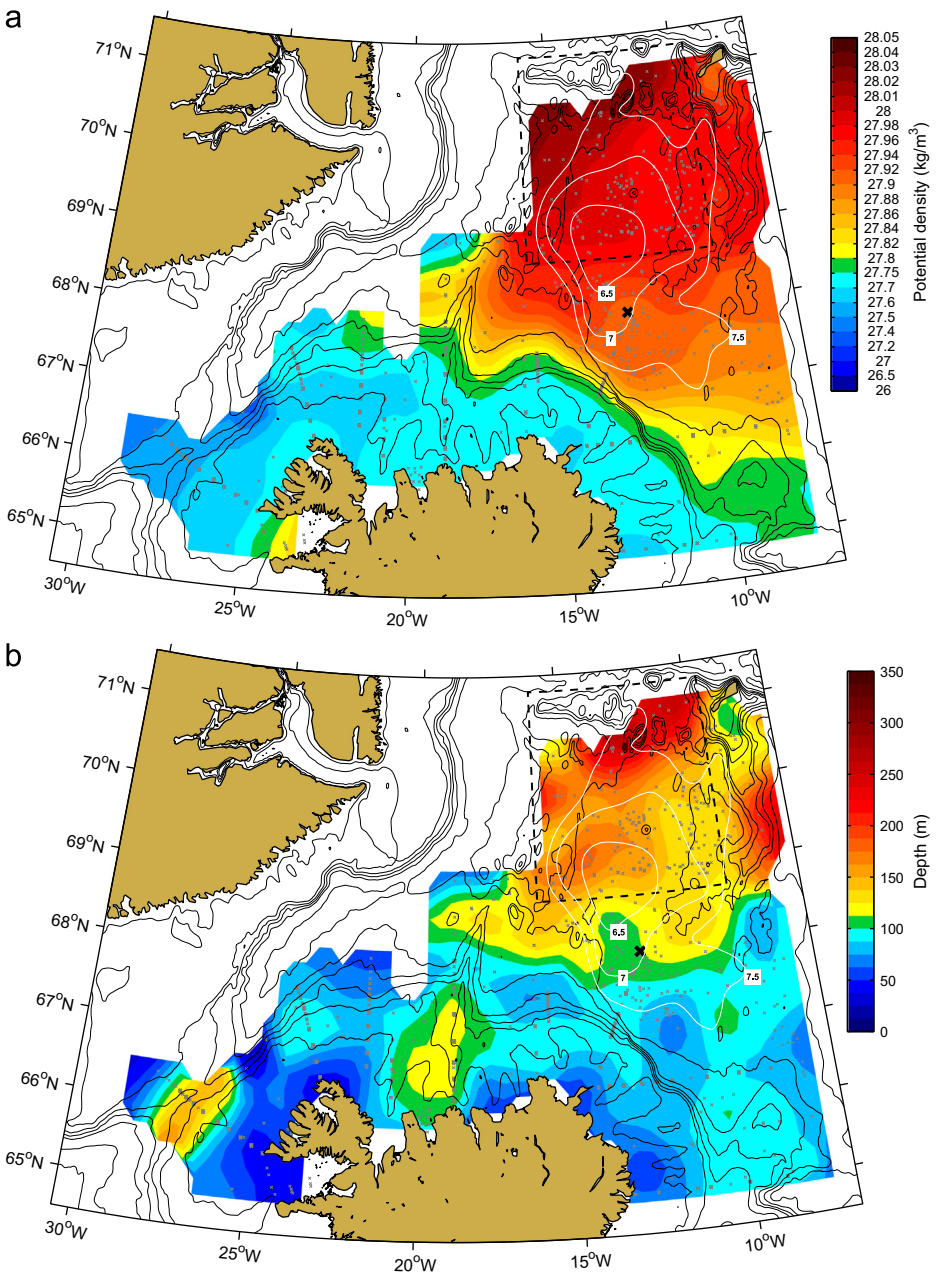

Fig. 2. Late-winter (February–April) mixed-layer potential density (a) and depth (b). The north-central Iceland Sea is outlined by the black dashed lines and the white lines are summer (May through October) contours of dynamic height of the surface relative to 500 db in units of dynamic cm (Våge et al., 2013). The gray crosses mark the locations of data points and the black cross represents the Langanes 6 repeat hydrographic station. The 200 m, 400 m, 600 m, 800 m, 1000 m, 1400 m, and 2000 m isobaths are contoured as black lines.

deep reference level was a near-uniform increase in summer (not shown). This is primarily caused by a change in steric height due to thermal expansion. The center position and shape of the gyre were qualitatively similar between the different seasons. These results are in accordance with Voet et al. (2010), who found a very weak seasonal signal in the circulation of the Iceland Sea Gyre.

4. Mixed-layer evolution in the north-central Iceland Sea

The densest and deepest late-winter mixed layers were recorded in the north-central part of the Iceland Sea (the area enclosed by the black dashed line in Fig. 2, which also contains the northern half of the gyre). To better understand the seasonal evolution of the upper part of the water column that actively takes part in wintertime convection, we examined the month-to-month change in mixed-layer properties in this region. During more than half of the year, from November through May, the potential density of the mixed layer exceeded $\sigma_\theta = 27.8$ kg/m^3 (Fig. 4a), and had thereby attained sufficient density to potentially contribute to the overflows from the Nordic Seas. The mixed-layer potential density and depth monotonically increased from November to March. While the hydrographic properties were largely uniform at the tail end of winter, the high variability in mixed-layer depth in April indicates that the onset of restratification tends to take place during that month (Fig. 4b). With abating levels of buoyancy and wind forcing as well as increasing insolation in spring, wintertime convection comes to a halt and a shallow, warm surface layer develops.

The seasonal evolution of the upper water column is evident also in Fig. 5 by increased near-surface densities and deeper mixed

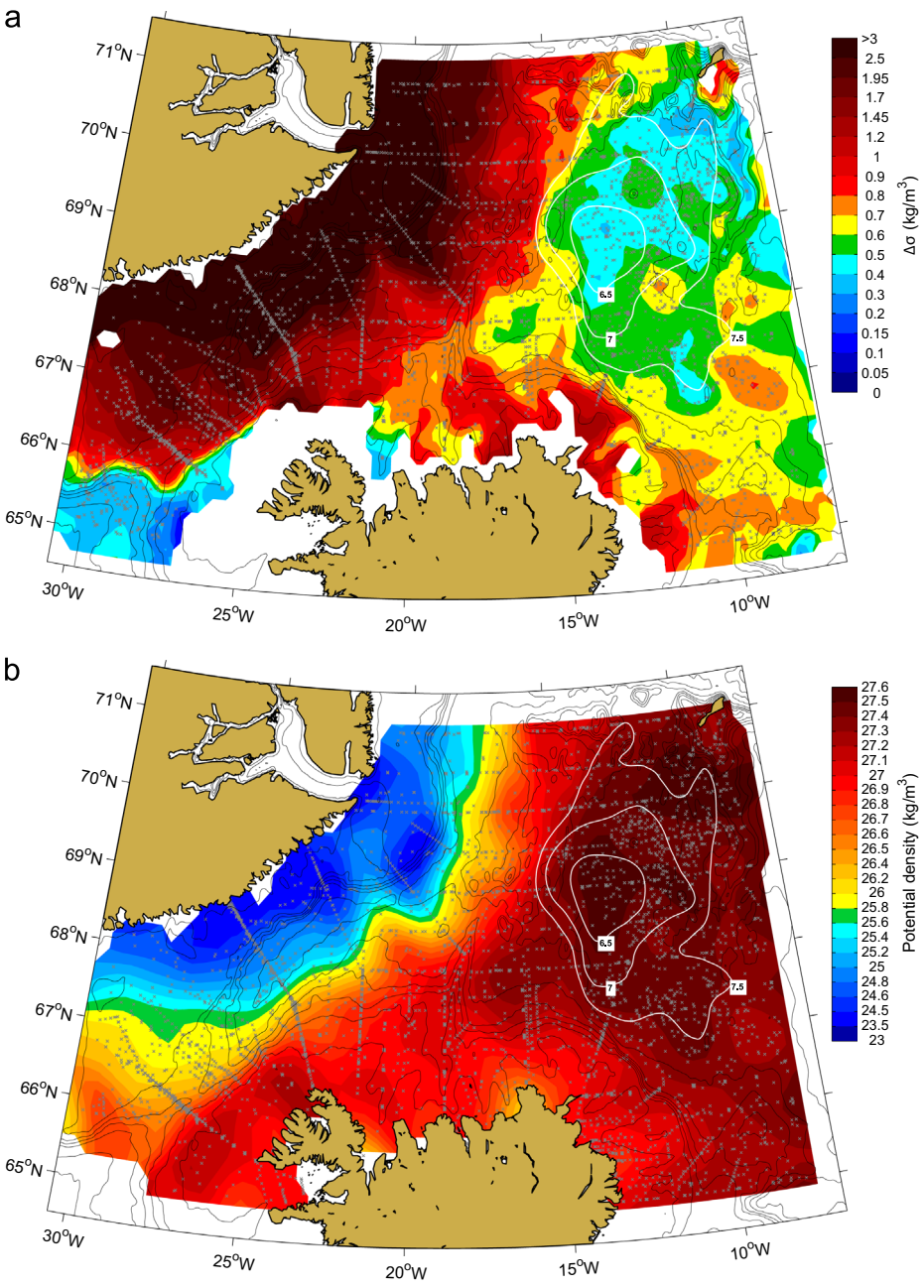

Fig. 3. Summer half-year (May–October) stratification (a, as the difference in potential density between 10 and 250 m) and potential density in the mixed layer (b). The white lines are contours of dynamic height of the surface relative to 500 db in units of dynamic cm (Våge et al., 2013), and the gray crosses mark the locations of data points. The 200 m, 400 m, 600 m, 800 m, 1000 m, 1400 m, and 2000 m isobaths are contoured as black lines.

layers in winter. While there is a trend of increasingly deep mixed layers during the course of each winter, it is clearly not as monotonic as suggested by Fig. 4b. This is due to the non-uniform spatial and temporal character of convection. In particular, mixed layers near the northern end of the domain were in general deeper than those farther south. Inter-annual variability in mixed-layer depth and potential density is clearly present as well. This is dominated by changes in the magnitude of the atmospheric forcing, but the stratification of the upper water column prior to the onset of wintertime convection also plays a role.

The mixed-layer evolution documented in Figs. 4 and 5 suggests that the $\sigma_\theta = 28.03$ kg/m^3 isopycnal is only on occasion ventilated in the Iceland Sea. In fact, only five of the late-winter profiles contained mixed layers with greater potential density, all of which came from Argo floats in the northern Iceland Sea in winter 2013. Våge et al. (2011) found that a substantial portion of the NIJ transport (0.6 ± 0.1 Sv) was of a density class exceeding $\sigma_\theta = 28.03$ kg/m^3 and hypothesized that it was fed by waters originating from overturning in the interior Iceland Sea. This begs the question: to what extent does the Iceland Sea provide the densest contribution to the NIJ and hence to the Denmark Strait overflow plume?

Data from one particular Argo float, documented for more than two years and corrected for drift in the conductivity and pressure sensors (Wong et al., 2003), may indicate that ventilation of waters denser than $\sigma_\theta = 28.03$ kg/m^3 is more prevalent than the few direct records of such dense mixed layers would suggest. The low values of potential vorticity in the upper water column in Fig. 6 indicate weak stratification associated with wintertime convection (e.g. Talley and McCartney, 1982). During its trajectory through the northern Iceland Sea in winter 2007–2008, the float encountered

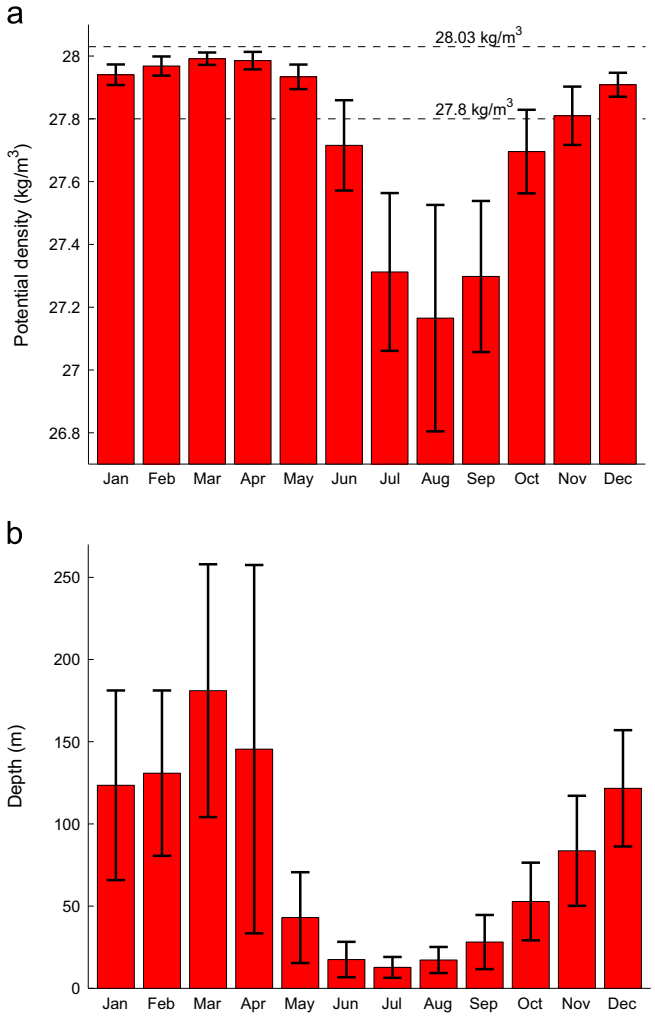

Fig. 4. Seasonal evolution of the mixed-layer potential density (a) and depth (b) within the north-central Iceland Sea area indicated in Fig. 2. The red bars and the vertical black lines represent the monthly means and standard deviations, respectively. (With sample sizes ranging from 41 in January to 190 in August, the standard error of the mean is very small for most months.) (For interpretation of the references to color in this figure caption, the reader is referred to the web version of this paper.)

mixed layers deeper than 300 m (isolated from the surface by early stages of restratification, but clearly formed during the same winter, see for example Våge et al., 2009). While neither this float nor any of the other profiles from winter 2007–2008 recorded mixed-layers denser than $\sigma_\theta = 28.03\ \mathrm{kg/m^3}$, the lens of weakly stratified water that was present for most of 2008 between 300 and 450 m and resulted from convection during that winter contained water that exceeded this density. This would imply that also waters that may feed the densest portion of the NIJ were ventilated in the Iceland Sea in winter 2007–2008. Indeed, a substantial number of the north-central Iceland Sea profiles (about 6%) had a potential vorticity of less than $8\ (\mathrm{ms})^{-1} \times 10^{-12}$ at the $\sigma_\theta = 28.03\ \mathrm{kg/m^3}$ isopycnal, implying that water of this density class may be ventilated on a more regular basis than the direct observations suggest.

5. Change in availability of dense water to the NIJ during the mid-1990s

The sparse amount of wintertime data prior to 2005 in the north-central Iceland Sea precludes a thorough investigation into the long-term variability in the ventilation of the densest waters transported by the NIJ. We examine instead the depth of the $\sigma_\theta = 28.03\ \mathrm{kg/m^3}$ isopycnal in the vicinity of the outermost station on the Langanes section off the north-east corner of Iceland (Langanes 6, black cross in Fig. 2) to shed light on the potential Iceland Sea source of dense water to the NIJ. The station is located within the southern part of the gyre, outside the region of most intense convection, and is typically sampled four times per year. It is very unlikely that this isopycnal was ventilated locally as there were no observed mixed layers with a potential density exceeding $27.97\ \mathrm{kg/m^3}$ and the $\sigma_\theta = 28.03\ \mathrm{kg/m^3}$ isopycnal was not observed at shallower depths than 250 m over the recorded period (Fig. 7).

The time series of isopycnal depth shown in Fig. 7 indicates that dense water was found higher in the water column at the beginning of the record and deeper toward the end. In particular, it appears that an abrupt change took place over only 2–3 years around the mid-1990s. Prior to 1995 the mean depth of the $\sigma_\theta = 28.03\ \mathrm{kg/m^3}$ isopycnal was approximately 60 m shallower than the following years. Such piecewise constant fits separated by a jump discontinuity across 1995 ± 1 year were statistically significant with confidence intervals exceeding the 99th percentile. This may be the result of a change in the convective activity in the Iceland Sea, a persistent change in the circulation of the Iceland Sea Gyre, or some combination of both, and has implications for the available supply of dense water to the NIJ.

6. Atmospheric forcing

In the early 1970s the NAO began a period that was characterized by a positive trend, i.e. a period during which there was a tendency for enhanced westerlies across the North Atlantic (Hurrell, 1995). This period persisted until the early 1990s, when the NAO entered a period where the trend became negative (Cohen and Barlow, 2005). The winters of 1994–1995 and 1995–1996 marked a particularly dramatic transition from a large positive NAO state to a large negative NAO state (Fig. 8a, Flatau et al., 2003). However, Cohen and Barlow (2005) note that the statistical significance of the trend of the NAO during both periods is generally not robust and highly dependent on the choice of start and end date. Fig. 8a also shows the linear least squares fit to the winter mean NAO index. The trend over the entire period is not statistically significant and, in agreement with Cohen and Barlow (2005), the trends before and after 1995 are not robust. In contrast, the transition in winter mean NAO index before and after 1995 from positive conditions to more neutral conditions was statistically significant at the 99th percentile confidence level using the aforementioned test that takes into account the temporal autocorrelation of geophysical time series. The choice of 1995 ± 1 year as a breakpoint resulted in a minimum in the root mean square error of the fit to the data. Regardless of how one characterizes the changes in NAO, i.e. as a linear trend or a jump discontinuity, this transition from positive to neutral NAO conditions has had a number of impacts on the subpolar North Atlantic. These include a reduction in the magnitude of the wind stress over the North Atlantic (Flatau et al., 2003) that has resulted in a weakening and warming of the subpolar gyre (Häkkinen and Rhines, 2004; Straneo and Heimbach, 2013). The impact of variability in the ILD on these processes has not been investigated. However, for the period from 1980 onwards an index of the ILD computed from the ERA-I indicates a weak negative trend (Fig. 8b), i.e. the Icelandic Low is becoming shallower at a faster rate than the Lofoten Low. However, the trend is not statistically significant at the 95th percentile confidence interval. The transition across 1995 ± 1 year, on the other hand, is statistically significant at the 95th percentile confidence level.

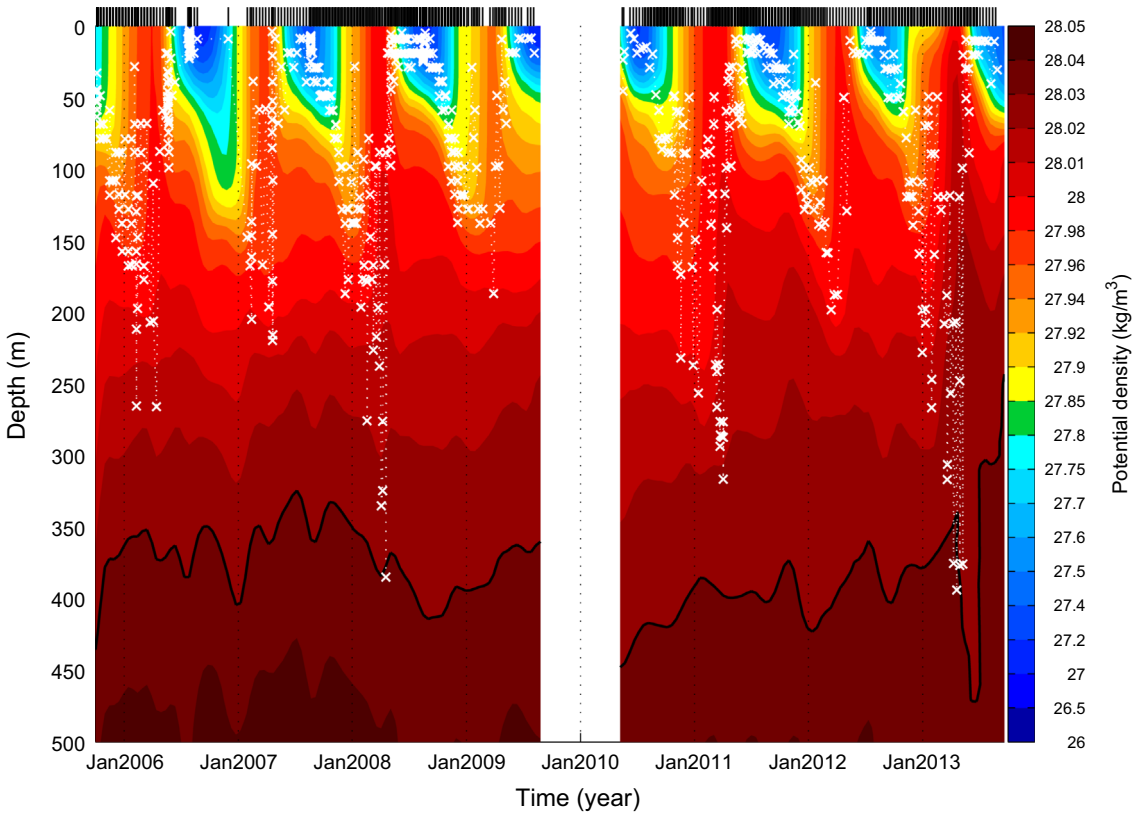

Fig. 5. Temporal evolution of potential density in the upper 500 m within the north-central Iceland Sea area indicated in Fig. 2. Each profile, denoted by a vertical bar along the top, is considered representative of this region. The white crosses indicate mixed-layer depths. The black contour is the $\sigma_\theta = 28.03$ kg/m^3 isopycnal.

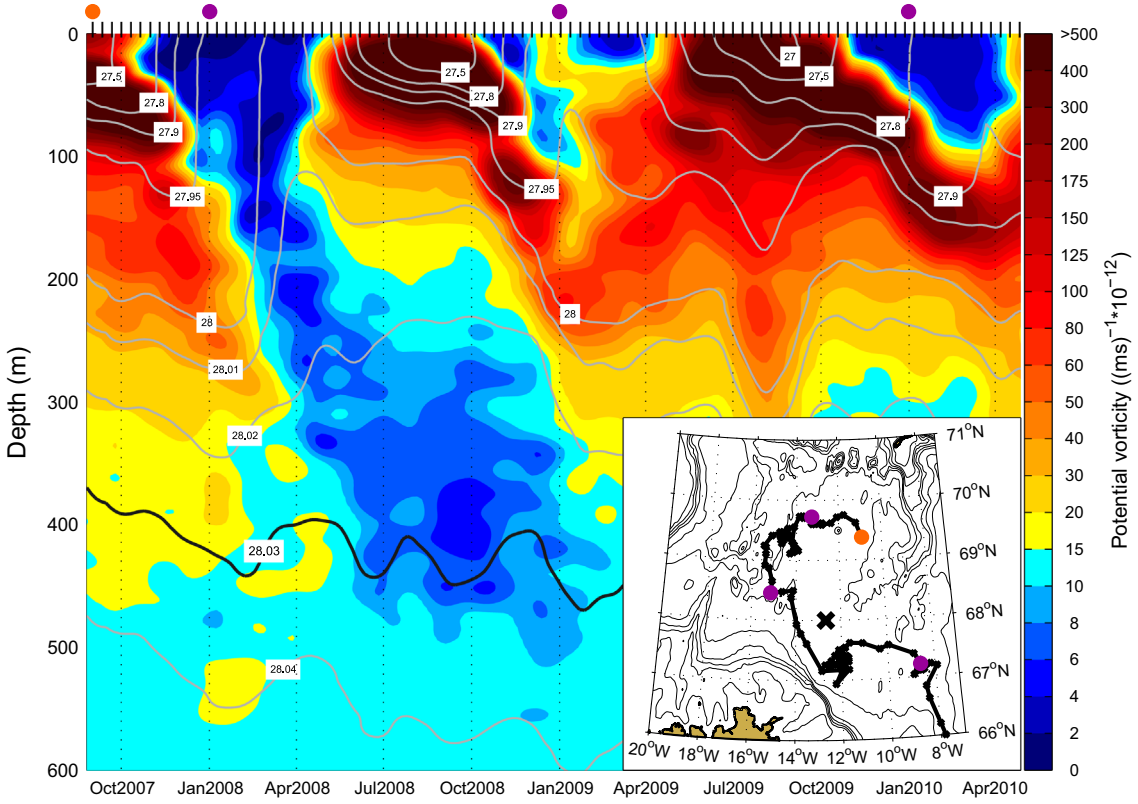

Fig. 6. Temporal evolution of potential vorticity (color, $(\mathrm{ms})^{-1} \times 10^{-12}$) and potential density (contours, kg/m^3) along the trajectory of Argo float 7900177 in the Iceland Sea. The vertical bars along the top denote the time of each profile. The inset shows the trajectory of the float. The orange and purple dots mark the float's deployment position and location at the beginning of each January, respectively, and the black cross represents the Langanes 6 repeat hydrographic station. The 200 m, 400 m, 600 m, 800 m, 1000 m, 1400 m, and 2000 m isobaths are contoured as black lines. (For interpretation of the references to color in this figure caption, the reader is referred to the web version of this paper.)

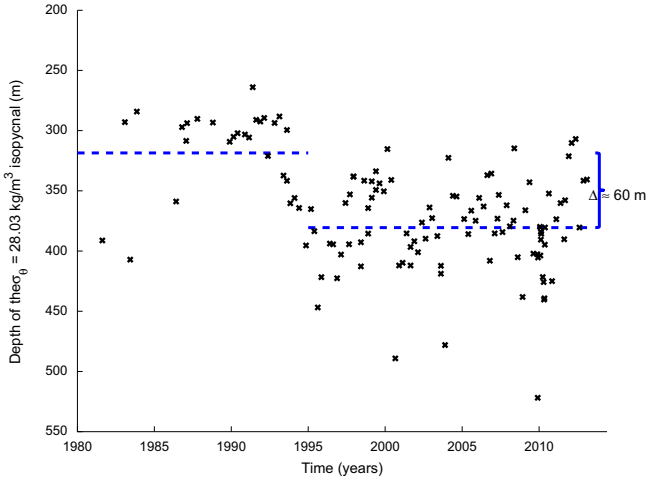

Fig. 7. Depth of the $\sigma_\theta = 28.03$ kg/m^3 isopycnal in the vicinity of the repeat station Langanes 6 indicated by the black cross in Fig. 2. The gray lines represent the means of the periods 1980–1995 and 1995–present.

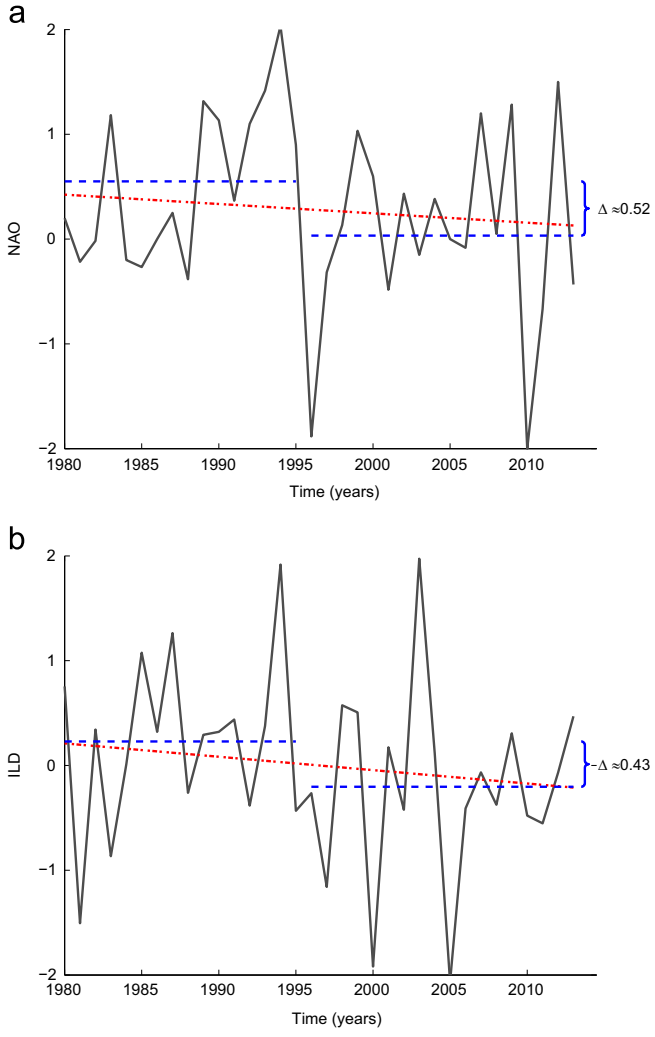

Fig. 8. Winter mean NAO (a) and ILD (b) indices. The red dotted lines represent the linear least squares fit to the data, while the blue dashed lines represent mean values before and after a breakpoint during the winter of 1994–1995. (For interpretation of the references to color in this figure caption, the reader is referred to the web version of this paper.)

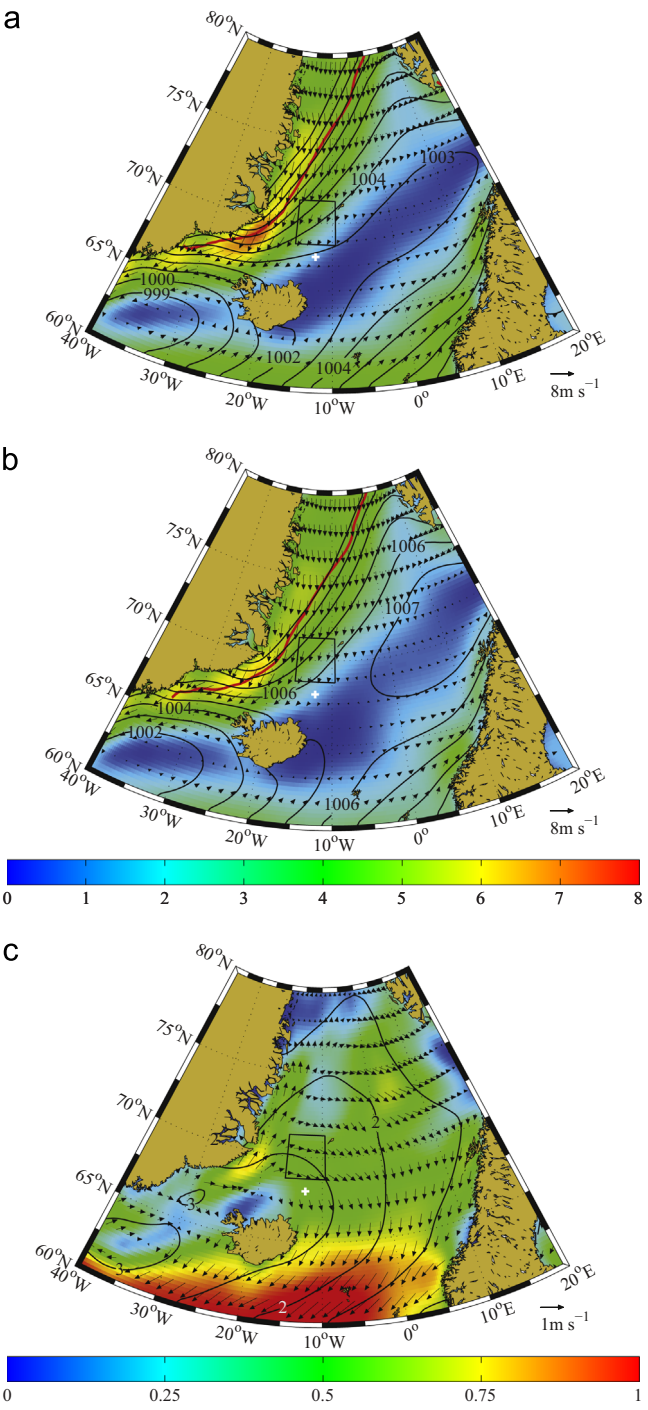

Fig. 9. Mean atmospheric circulation over the Nordic Seas during winter (November through April) for the period 1980–1995 (a), the period 1996–2013 (b), and the difference between the periods (i.e. the 1996–2013 mean minus the 1980–1995 mean, c). The sea-level pressure (contours, mb) and 10 m winds (color and vectors, m/s) are shown. The north-central Iceland Sea region is outlined by the black dashed lines and the location of the Langanes 6 station is indicated by the white cross. The thick red curve in (a) and (b) denotes the 50% sea ice concentration contour during the respective period. All data are from the ERA-I reanalysis. (For interpretation of the references to color in this figure caption, the reader is referred to the web version of this paper.)

The winter mean (November through April) ERA-I sea-level pressure and 10 m wind field for the periods 1980–1995 and 1996–2013 as well as the difference between the winter means for the two periods (i.e. the mean over 1996–2013 minus the mean over 1980–1995) across the Nordic Seas are shown in Fig. 9. The

increase in pressure between the two periods is the result of the weakening of the Icelandic and Lofoten Lows and is consistent with the behavior of both the NAO and the ILD over this period. The result is a pronounced reduction in the magnitude of the winter mean 10 m winds along the Denmark Strait as well as over the Iceland Sea. The difference between the two periods is therefore characterized by an anti-cyclonic circulation anomaly across the Iceland Sea.

Elevated sea to air heat fluxes over the Iceland Sea (here we will use the convention that heat fluxes out of the ocean are positive) are associated with strong northerly flow (Moore et al., 2012), and hence the change in behavior of the atmospheric circulation identified in Fig. 9 should result in a decrease in the magnitude of the sea to air heat fluxes over the region. Time series of winter mean turbulent sea to air heat flux, the sum of the sensible and latent heat fluxes, averaged over the north-central Iceland Sea confirm this decline (Fig. 10a). The curl of the wind stress is positive over the central Iceland Sea with a narrow band of anti-cyclonic wind stress along the coast that is the result of lower wind speeds over the sea ice and near coastal regions (Malmberg and Jónsson, 1997; Våge et al., 2013). The wind stress curl also exhibits a considerable amount of inter-annual variability (Fig. 10b, Malmberg and Jónsson, 1997) that is also most likely regulated by the ILD. Consistent with Flatau et al. (2003) and Moore et al. (2012), both the winter mean turbulent heat flux and the wind stress curl have a negative trend, as determined from a linear least squares fit, over the period 1980–2013. However, only the trend in the turbulent heat flux is statistically significant at the 95th percentile confidence interval (Rudnick and Davis, 2003; Moore, 2012). Also shown in Fig. 10 are piecewise constant fits to the time series with a breakpoint in 1995. Both time series can also be characterized by a jump discontinuity across 1995. The statistical significance of the magnitude of the jump was also considered using an equivalent test. In this case, the magnitude of jump was statistically significant at the 95th percentile confidence interval for both time series. The root mean square error for the jump discontinuity fit to the data was in both cases smaller than that for the linear least squares fit, suggesting that the former provides a better fit to the data. The difference in the characterization of the low frequency variability of the heat flux time series in this paper with that in Moore et al. (2015) can be attributed to averaging over different spatial regions.

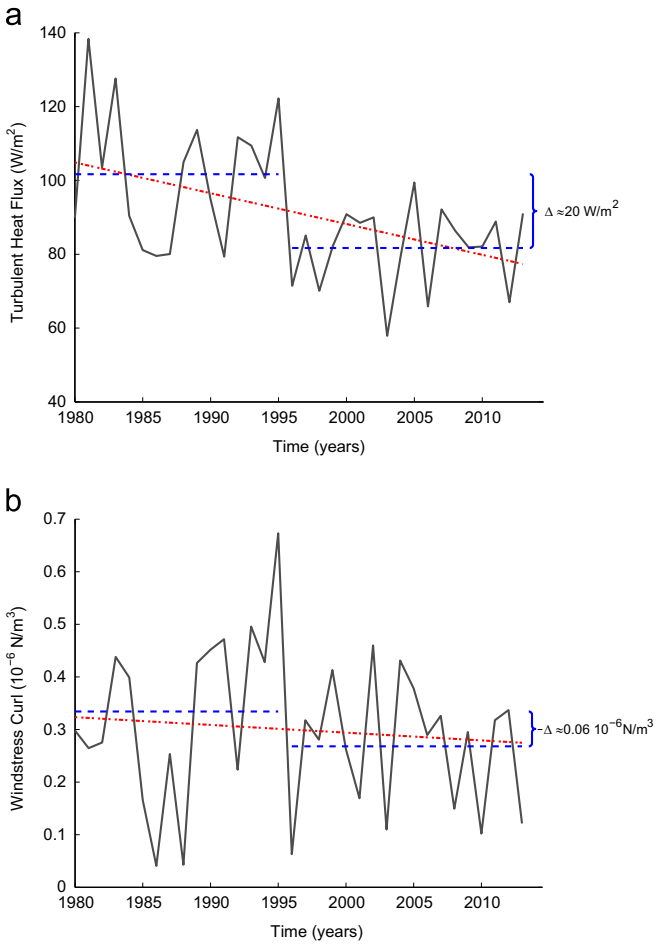

Fig. 10. Winter mean total turbulent heat flux (a) and wind stress curl (b) for the north-central Iceland Sea region. The red dotted lines represent the linear least squares fit to the data, while the blue dashed lines represent mean values before and after a breakpoint during the winter of 1994–1995. (For interpretation of the references to color in this figure caption, the reader is referred to the web version of this paper.)

The correlations of the winter mean turbulent heat flux and wind stress curl time series with the corresponding indices of NAO and ILD as well as the sea-level pressures associated with the Icelandic and Lofoten Lows were calculated. They are generally consistent with the idea that the Lofoten Low is an important contributor to the variability observed in both time series, with the Icelandic Low also playing an important role only in the variability observed in the wind stress curl (Table 1).

Moore et al. (2015) attributed the trend in the turbulent heat flux time series to a reduction in the air–sea temperature difference over the region as well as to a retreat of the sea ice off the east coast of Greenland. These previous results do not address the changes in the occurrence or structure of the extreme heat flux events that result in this winter mean behavior. This is important because of the impact that the high heat flux events have on the total loss of heat from the ocean over a typical winter. For example, events where the turbulent heat flux exceeds the 90th percentile value contribute over 35% of the total winter heat loss. Fig. 11 shows the time series of occurrence frequency of extreme turbulent heat fluxes over the north-central Iceland Sea, defined as the number of times that the turbulent heat flux exceeded the 90th and 10th percentile values based on all winter values over the period 1980–2013. These values are 246 and −15 W/m^2, respectively. The occurrence of high heat flux events has been decreasing over this period while the occurrence of events where there was a net warming of the ocean surface have been increasing. This behavior is consistent with the changes in the winter mean circulation (Fig. 9) which indicate a trend towards weaker northerly flow into the Iceland Sea since 1980.

The sea to air heat fluxes tend to be highest at the ice edge, where the cold and dry Arctic air first comes in contact with relatively warm surface waters (Marshall et al., 1998; Renfrew and Moore, 1999). As a result, the recent retreat of the sea ice from the vicinity of the Iceland Sea (Strong, 2012; Moore et al., 2015) is also expected to result in a reduction of the magnitude of the sea to air heat fluxes over the Iceland Sea. To confirm this behavior, all events where the turbulent heat flux exceeded the 90th percentile value, 246 W/m^2, were identified for the first and last 10 years of

Table 1
Correlation coefficients of the winter mean turbulent heat flux and wind stress curl over the north-central Iceland Sea with various indices of the large-scale circulation over the subpolar North Atlantic. Correlations that are underlined are statistically significant at the 95th percentile confidence interval, while those that are bold are statistically significant at the 99th percentile confidence interval.

	NAO	ILD	Icelandic Low	Lofoten Low
Turbulent heat flux	0.30	**−0.37**	−0.27	**−0.60**
Curl of the wind stress	**0.63**	−0.08	**0.60**	**0.67**

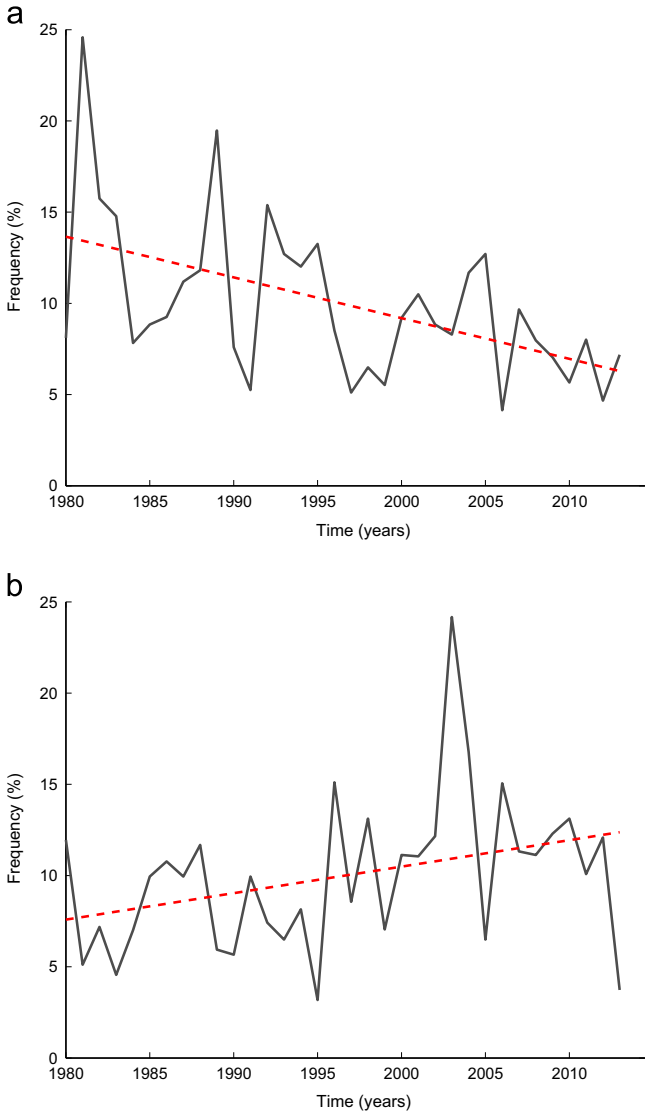

Fig. 11. Frequency of occurrence of total turbulent heat fluxes greater than the 90th percentile total turbulent heat flux (a) and less than the 10th percentile total turbulent heat flux (b) at the middle of the north-central Iceland Sea region.

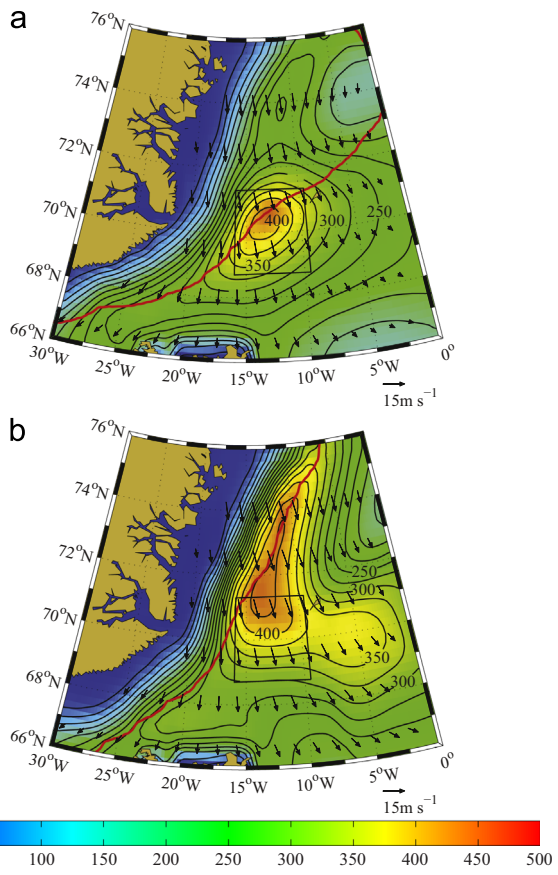

Fig. 12. Composite mean high heat flux events at the middle of the north-central Iceland Sea region during 1980–1989 from 75 events (a) and 2004–2013 from 65 events (b). The thick red line represents the composite 50% sea ice concentration contour. (For interpretation of the references to color in this figure caption, the reader is referred to the web version of this paper.)

the period of interest, i.e. 1980–1989 and 2004–2013 (Fig. 12). The retreat of the sea ice has resulted in a northward shift of the region of the largest heat fluxes away from the north-central Iceland Sea and a narrowing of the marginal ice zone (Strong, 2012). The spatial distribution of the heat fluxes between the two periods reflects this narrowing. In particular, during the earlier period when the marginal ice zone was broad, the heat fluxes were significant over a large region, while during the latter period, characterized by a narrow marginal ice zone, there was a much tighter gradient to the heat flux. This northward transition of the maximum in the heat fluxes would result in a reduction in the magnitude of the atmospheric forcing of oceanic convection over the Iceland Sea.

7. Discussion and conclusions

Waters of sufficient potential density to feed the overflows across the Greenland-Scotland Ridge are formed throughout the Iceland Sea in winter. Its contribution to the overflows could be on the order of 2 Sv, a considerable fraction of the total overflow of about 6 Sv (Østerhus et al., 2008). The densest waters are formed in the northern part of the Iceland Sea, on the outskirts of the cyclonic gyre. This is primarily dictated by closer proximity to the ice edge and stronger atmospheric forcing there, as the water column is more preconditioned for overturning near the center of the gyre. Swift and Aagaard (1981) suggested that an inflow of saline Atlantic Water south of Jan Mayen from the Norwegian Sea could also play a role.

The wintertime formation of dense water outside the center of the gyre does not appear to have a lasting impact on its structure, but could have ramifications on the residence time of this product and its export from the Iceland Sea. Specifically, dense water located outside the center of the gyre is more accessible to boundary currents, such as the NIJ, and can therefore more readily supply the overflows. This is consistent with the low residence time north of the Greenland-Scotland Ridge estimated for the Arctic-origin overflow water (Smethie and Swift, 1989).

The NIJ provides the densest contribution ($\sigma_\theta \geq 28.03$ kg/m^3) to the Denmark Strait overflow plume and is hypothesized to be part of an interior overturning loop that involves water mass transformation in the central Iceland Sea (Våge et al., 2011). However, only a minor fraction (2%) of the 1980 to present late-winter profiles from the north-central Iceland Sea recorded such dense mixed layers. A lens of weakly stratified water resulting from overturning in winter 2007–2008 was revealed by an Argo float transiting through the northern Iceland Sea. The lens included waters denser than $\sigma_\theta = 28.03$ kg/m^3, implying that this isopycnal had been ventilated that winter even though direct observations are lacking. Low values of potential vorticity at this deep isopycnal suggest that water of this density class may be

ventilated more often than direct observations of dense mixed layers indicate. Given a large temporal and spatial variability in convection, it is likely that the data set used in this study is too sparse to ensure reliable direct detection of the most intense convective episodes each winter.

It is also possible that convection in the Iceland Sea has become less intense over the past two decades. A deepening of the $\sigma_\theta = 28.03$ kg/m^3 isopycnal in the vicinity of the repeat Langanes 6 station (its location is marked on Fig. 2) may indicate a decrease in the available supply of the NIJ's densest component. While the only mixed layers denser than $\sigma_\theta = 28.03$ kg/m^3 were observed in early 2013, the very sparse winter measurements prior to the deployment of Argo floats in 2005 revealed near-surface waters that had attained similar densities also in early 1981. Swift and Aagaard (1981) found densities in the near-surface layer exceeding 28 kg/m^3 using hydrographic data obtained from late February/early March in 1975, and surmised that by the end of that winter the density could have reached 28.05 kg/m^3. Such a decline in the convective activity was hypothesized by Moore et al. (2015). They documented a trend of diminished wintertime atmospheric forcing and conducted simulations with a one-dimensional mixed-layer model that predicted a concomitant reduction in convection. Over time, the result would likely lead to a weakening of the overturning loop that feeds the NIJ and hence result in a decreased supply of the densest overflow waters to the AMOC.

The time series of winter mean sea to air heat flux and wind stress curl over the north-central Iceland Sea (Fig. 10) are consistent with this interpretation. Both show a long-term decline that would lead to a reduction in the buoyancy flux from the ocean to the atmosphere as well as a reduction in the doming of the isopycnals of the Iceland Sea Gyre. The diminished occurrence frequency of high heat flux events over the region (Fig. 11) as well as a northward shift in the location of the heat flux maximum (Fig. 12) contribute to the reduction in the buoyancy flux. There is evidence of a step-like discontinuity in both the turbulent heat flux and wind stress curl time series around 1995 that is consistent with the observed long-term behavior of the depth of the $\sigma_\theta = 28.03$ kg/m^3 isopycnal (Fig. 7). The timing of these discontinuities is simultaneous with the transition from NAO positive to NAO neutral conditions (Flatau et al., 2003; Cohen and Barlow, 2005) that resulted in a number of other changes in the oceanography of the region (e.g. Häkkinen and Rhines, 2004; Pálsson et al., 2012; Straneo and Heimbach, 2013). However, the muted dependence of the air–sea forcing over this region on the depth of the Icelandic Low as compared to the Lofoten Low (Table 1) suggests that further work is required in order to understand the relative importance of large-scale atmospheric circulation patterns like the NAO and ILD to the climate of the Nordic Seas.

Recent studies have placed a renewed emphasis on the Iceland Sea and strongly suggest that it provides a more important contribution to the AMOC than previously thought. While the present hydrographic data set is too sparse to provide a definitive account of the Iceland Sea's recent convective history, in particular as regards its potential to supply the densest component of the NIJ, there is evidence that also these waters can be locally ventilated. Additional wintertime measurements will continue to shed light on the water mass transformation in the Iceland Sea as a source of dense water to the NIJ, which will clarify the importance of the Iceland Sea in the North Atlantic climate system.

Acknowledgments

The authors would like to thank Bob Pickart for comments to an early version of the manuscript. Support for this work was provided by the Norwegian Research Council under Grant agreement no. 231647 (KV), the European Union 7th Framework Programme (FP7 2007-2013) under Grant agreement no. 308299 NACLIM Project (K.V., S.J., and H.V.), and the Natural Sciences and Engineering Research Council of Canada (K.M.).

References

Cohen, J., Barlow, M., 2005. The NAO, the AO, and global warming: how closely related?##J. Clim. 18, 4498–4513.
Dee, D.P., Uppala, S.M., Simmons, A.J., Berrisford, P., Poli, P., et al., 2011. The ERA-Interim reanalysis: configuration and performance of the data assimilation system. Q. J. R. Meteorol. Soc. 137, 553–597. http://dx.doi.org/10.1002/qj.828.
Dickson, R.R., Brown, J., 1994. The production of North Atlantic Deep Water: sources, rates and pathways. J. Geophys. Res. 99, 12319–12341.
Dickson, R.R., Lamb, H.H., Malmberg, S.-A., Colebrook, J.M., 1975. Climatic reversal in northern North Atlantic. Nature 256, 479–482.
Eldevik, T., Nilsen, J.E.Ø., Iovino, D., Olsson, K.A., Sandø, A.B., Drange, H., 2009. Observed sources and variability of Nordic Seas overflow. Nat. Geosci. 2, 406–410. http://dx.doi.org/10.1038/NGEO518.
Flatau, M.K., Talley, L., Niiler, P.P., 2003. The North Atlantic Oscillation, surface current velocities, and SST changes in the subpolar North Atlantic. J. Clim. 16, 2355–2369.
Fogelqvist, E., Blindheim, J., Tanhua, T., Østerhus, S., Buch, E., Rey, F., 2003. Greenland-Scotland overflow studied by hydro-chemical multivariate analysis. Deep Sea Res. I 50, 73–102.
Gebbie, G., Huybers, P., 2010. Total matrix intercomparison: a method for determining the geometry of water-mass pathways. J. Phys. Oceanogr. 40, 1710–1728. http://dx.doi.org/10.1175/2010JPO4272.1.
Häkkinen, S., Rhines, P.B., 2004. Decline of subpolar North Atlantic circulation during the 1990s. Science 304, 555–559.
Hansen, B., Østerhus, S., 2000. North Atlantic–Nordic Seas exchanges. Progr. Oceanogr. 45, 109–208.
Harden, B.E., Renfrew, I.A., Petersen, G.N., 2011. A climatology of wintertime barrier winds off southeast Greenland. J. Clim. 24, 4701–4717. http://dx.doi.org/10.1175/2011JCLI4113.1.
Holfort, J., Albrecht, T., 2007. Atmospheric forcing of salinity in the overflow of Denmark Strait. Ocean Sci. 3, 411–416.
Hurrell, J.W., 1995. Decadal trends in the North Atlantic Oscillation: regional temperatures and precipitation. Science 269, 676–679.
Hurrell, J.W., Deser, C., 2009. North Atlantic climate variability: the role of the North Atlantic Oscillation. J. Mar. Syst. 78, 28–41.
Jahnke-Bornemann, A., Bruemmer, B., 2009. The Iceland-Lofoten pressure difference: different states of the North Atlantic low-pressure zone. Tellus 61, 466–475. http://dx.doi.org/10.1111/j.1600-0870.2009.00401.x.
Jeansson, E., Jutterström, S., Rudels, B., Anderson, L.G., Olsson, K.A., Jones, E.P., Smethie Jr., W.M., Swift, J.H., 2008. Sources to the East Greenland Current and its contribution to the Denmark Strait overflow. Progr. Oceanogr. 78, 12–28. http://dx.doi.org/10.1016/j.pocean.2007.08.031.
Jochumsen, K., Quadfasel, D., Valdimarsson, H., Jónsson, S., 2013. Variability of the Denmark Strait overflow: moored time series from 1996–2011. J. Geophys. Res. 117, C12003. http://dx.doi.org/10.1029/2012JC008244.
Jónsson, S., 1992. Sources of fresh water in the Iceland Sea and the mechanisms governing its interannual variability. ICES Mar. Sci. Symp. 195, 62–67.
Jónsson, S., 1999. The Circulation in the Northern Part of the Denmark Strait and its Variability. ICES Report CM-1999/L:06, 9 pp.
Jónsson, S., 2007. Volume flux and fresh water transport associated with the East Icelandic Current. Progr. Oceanogr. 73, 231–241. http://dx.doi.org/10.1016/j.pocean.2006.11.003.
Jónsson, S., Valdimarsson, H., 2004. A new path for the Denmark Strait overflow water from the Iceland Sea to Denmark Strait. Geophys. Res. Lett. 31, L03305. http://dx.doi.org/10.1029/2003GL019214.
Kelly, P.M., Goodess, C.M., Cherry, B.S.G., 1987. The interpretation of the Icelandic sea ice record. J. Geophys. Res. 92, 10835–10843.
Köhl, A., 2010. Variable source regions of Denmark Strait and Faroe Bank Channel overflow waters. Tellus 62A, 551–568. http://dx.doi.org/10.1111/j.1600-0870.2010.00454.x.
Livingston, H.D., Swift, J.H., Östlund, H.G., 1985. Artificial radionuclide tracer supply to the Denmark Strait overflow between 1972 and 1981. J. Geophys. Res. 90, 6971–6982.
Logemann, K., Ólafsson, J., Snorrason, Á., Valdimarsson, H., Marteinsdóttir, G., 2013. The circulation of Icelandic waters—a modelling study. Ocean Sci. 9, 931–955. http://dx.doi.org/10.5194/os-9-931-2013.
Lorbacher, K., Dommenget, D., Niiler, P.P., Köhl, A., 2006. Ocean mixed layer depth: a subsurface proxy of ocean–atmosphere variability. J. Geophys. Res. 111, C07010. http://dx.doi.org/10.1029/2003JC002157.
Malmberg, S.-A., Jónsson, S., 1997. Timing of deep convection in the Greenland and Iceland Seas. ICES J. Mar. Sci. 54, 300–309.
Marshall, J., Dobson, F., Moore, G., Rhines, P., Visbeck, M., et al., 1998. The labrador sea deep convection experiment. Bull. Am. Meteorol. Soc. 79, 2033–2058.
Marshall, J., Schott, F., 1999. Open-ocean convection: observations, theory, and models. Rev. Geophys. 37, 1–64.

Mauritzen, C., 1996. Production of dense overflow waters feeding the North Atlantic across the Greenland-Scotland Ridge. Part 1: evidence for a revised circulation scheme. Deep Sea Res. I 43, 769–806.
Meincke, J., 1978. On the distribution of low salinity intermediate water around the Faroes. Dtsch. Hydrogr. Z. 31, 50–64.
Meincke, J., 1983. The modern current regime across the Greenland Scotland Ridge. In: Bott, M.H.P., Saxov, S., Talwani, M., Thiede, J. (Eds.), Structure and Development of the Greenland Scotland Ridge, New Methods and Concepts. Plenum Press, New York, pp. 637–650.
Moore, G.W.K., 2012. Decadal variability and a recent amplification of the summer Beaufort Sea High. Geophys. Res. Lett. 39, http://dx.doi.org/10.1029/2012GL051570.
Moore, G.W.K., Renfrew, I.A., Pickart, R.S., 2012. Spatial distribution of air–sea heat fluxes over the sub-polar North Atlantic Ocean. Geophys. Res. Lett. 39, L18806. http://dx.doi.org/10.1029/2012GL053097.
Moore, G.W.K., Straneo, F., Oltmanns, M., 2014. Trend and interannual variability in southeast Greenland Sea Ice: Impacts on coastal Greenland climate variability. Geophys. Res. Lett. 41, 8619–8626. http://dx.doi.org/10.1002/2014GL062107.
Moore, G.W.K., Våge, K., Pickart, R.S., Renfrew, I.A., 2015. Open-ocean convection becoming less intense in the Greenland and Iceland Seas. Nat. Clim. Change, in revision.
Nilsen, J.E.Ø., Falck, E., 2006. Variations of mixed layer properties in the Norwegian Sea for the period 1948–1999. Progr. Oceanogr. 70, 58–90. http://dx.doi.org/10.1016/j.pocean.2006.03.014.
Olsson, K.A., Jeansson, E., Tanhua, T., Gascard, J.-C., 2005. The East Greenland Current studied with CFCs and released sulphur hexafluoride. J. Mar. Syst. 55, 77–95.
Østerhus, S., Sherwin, T., Quadfasel, D., Hansen, B., 2008. The overflow transport east of Iceland. In: Dickson, R.R., Meincke, J., Rhines, P. (Eds.), Arctic-Subarctic Ocean Fluxes: Defining the Role of the Northern Seas in Climate. Springer, Dordrecht, The Netherlands, pp. 427–441.
Pálsson, Ó.K., Gislason, A., Gudhfinsson, H.G., Gunnarsson, B., Ólafsdóttir, S.R., Petursdottir, H., Sveinbjörnsson, S., Thorisson, K., Valdimarsson, H., 2012. Ecosystem structure in the Iceland Sea and recent changes to the capelin (Mallotus villosus) population. ICES J. Mar. Sci. 69 (7), 1242–1254. http://dx.doi.org/10.1093/icesjms/fss071.
Perkins, H., Hopkins, T.S., Malmberg, S.-A., Poulain, P.-M., Warn-Varnas, A., 1998. Oceanographic conditions east of Iceland. J. Geophys. Res. 103, 21531–21542.
Pickart, R.S., Torres, D.J., Clarke, R.A., 2002. Hydrography of the Labrador Sea during active convection. J. Phys. Oceanogr. 32, 428–457.
Renfrew, I.A., Moore, G.W.K., 1999. An extreme cold-air outbreak over the Labrador Sea: roll vortices and air–sea interaction. Mon. Weather Rev. 127, 2379–2394.
Renfrew, I.A., Petersen, G.N., Sproson, D.A.J., Moore, G.W.K., Adiwidjaja, H., Zhang, S., North, R., 2009. A comparison of aircraft-based surface-layer observations over Denmark Strait and the Irminger Sea with meteorological analyses and QuikSCAT winds. Q. J. R. Meteorol. Soc. 135, 2046–2066. http://dx.doi.org/10.1002/qj.444.
Rhines, P.B., Häkkinen, S., Josey, S.A., 2008. Is oceanic heat transport significant in the climate system?. In: Dickson, R.R., Meincke, J., Rhines, P. (Eds.), Arctic-Subarctic Ocean Fluxes: Defining the Role of the Northern Seas in Climate. Springer, Dordrecht, The Netherlands, pp. 87–109.
Rudels, B., Eriksson, P., Buch, E., Budéus, G., Fahrbach, E., Malmberg, S.-A., Meincke, J., Mälkki, P., 2003. Temporal switching between sources of the Denmark Strait overflow water. ICES Mar. Sci. Symp. 219, 319–325.
Rudels, B., Fahrbach, E., Meincke, J., Budéus, G., Eriksson, P., 2002. The East Greenland Current and its contribution to the Denmark Strait overflow. ICES J. Mar. Sci. 59, 1133–1154.
Rudnick, D.L., Davis, R.E., 2003. Red noise and regime shifts. Deep Sea Res. I 50, 691–699.
Serreze, M.C., Carse, F., Barry, R.G., Rogers, J.C., 1997. Icelandic low cyclone activity: climatological features, linkages with the NAO, and relationships with recent changes in the Northern Hemisphere circulation. J. Clim. 10, 453–464.
Smethie Jr., W.M., Swift, J.H., 1989. The Tritium: Krypton-85 age of Denmark strait overflow water and gibbs fracture zone water just south of the Denmark Strait. J. Geophys. Res. 94, 8265–8275.
Stefánsson, U., 1962. North Icelandic waters. Rit Fiskid. 3, 1–269.
Straneo, F., Heimbach, P., 2013. North Atlantic warming and the retreat of Greenland's outlet glaciers. Nature 504, 36–43. http://dx.doi.org/10.1038/nature12854.
Strong, C., 2012. Atmospheric influence on Arctic marginal ice zone position and width in the Atlantic sector, February–April 1979–2010. Clim. Dyn. 39, 3091–3102. http://dx.doi.org/10.1007/s00382-012-1356-6.
Swift, J.H., Aagaard, K., 1981. Seasonal transitions and water mass formation in the Iceland and Greenland Seas. Deep Sea Res. 28A, 1107–1129.
Swift, J.H., Aagaard, K., Malmberg, S.-A., 1980. The contribution of the Denmark Strait overflow to the deep North Atlantic. Deep Sea Res. 27A, 29–42.
Talley, L.D., McCartney, M.S., 1982. Distribution and circulation of Labrador Sea Water. J. Phys. Oceanogr. 12, 1189–1205.
Tanhua, T., Olsson, K.A., Jeansson, E., 2005. Formation of Denmark Strait overflow water and its hydro-chemical composition. J. Mar. Syst. 57, 264–288.
Tanhua, T., Olsson, K.A., Jeansson, E., 2008. Tracer evidence of the origin and variability of Denmark Strait Overflow Water. In: Dickson, R.R., Meincke, J., Rhines, P. (Eds.), Arctic–Subarctic Ocean Fluxes: Defining the Role of the Northern Seas in Climate. Springer, Dordrecht, The Netherlands, pp. 475–503.
Våge, K., Pickart, R.S., Spall, M.A., Moore, G.W.K., Valdimarsson, H., Torres, D.J., Erofeeva, S.Y., Nilsen, J.E.Ø., 2013. Revised circulation scheme north of the Denmark Strait. Deep Sea Res. I 79, 20–39. http://dx.doi.org/10.1016/j.dsr.2013.05.007.
Våge, K., Pickart, R.S., Spall, M.A., Valdimarsson, H., Jónsson, S., Torres, D.J., Østerhus, S., Eldevik, T., 2011. Significant role of the North Icelandic Jet in the formation of Denmark Strait Overflow Water. Nat. Geosci. 4, 723–727. http://dx.doi.org/10.1038/NGEO1234.
Våge, K., Pickart, R.S., Thierry, V., Reverdin, G., Lee, C.M., Petrie, B., Agnew, T.A., Wong, A., Ribergaard, M.H., 2009. Surprising return of deep convection to the subpolar North Atlantic Ocean in winter 2007–2008. Nat. Geosci. 2, 67–72. http://dx.doi.org/10.1038/NGEO382.
Voet, G., Quadfasel, D., Mork, K.A., Søiland, H., 2010. The mid-depth circulation of the Nordic Seas derived from profiling float observations. Tellus 62, 516–529. http://dx.doi.org/10.1111/j.1600-0870.2010.00444.x.
Wernli, H., Schwierz, C., 2006. Surface cyclones in the ERA-40 dataset (1958–2001), Part I: novel identification method and global climatology. J. Atmos. Sci. 63, 2486–2507.
Wong, A.P.S., Johnson, G.C., Owens, W.B., 2003. Delayed-mode calibration of autonomous CTD float profiling salinity data by θ–S climatology. J. Atmos. Ocean. Technol. 20, 308–318.
Yang, J., Pratt, L.J., 2014. Some dynamical constraints on upstream pathways of the Denmark Strait overflow. J. Phys. Oceanogr. 44, 3033–3053. http://dx.doi.org/10.1175/JPO-D-13-0227.1.